The conductance of a linear chain: elastic and inelastic scattering effects

1992 J. Phys.: Condens. Matter 4 5309

(http://iopscience.iop.org/0953-8984/4/23/008)

J. Phys.: Condens. Matter 4 (1992) 5309–5326. Printed in the UK

The conductance of a linear chain: elastic and inelastic scattering effects

P L Pernas, F Flores and E V Anda

Departamento de Física de la Materia Condensada C-XII. Facultad de Ciencias, Universidad Autónoma, E-28049 Madrid, Spain

Received 30 December 1991

Abstract. The electronic transport properties of a linear chain have been analysed. The chain conductance, the electrochemical potential variations along the chain, and some defect scattering effects have been discussed using the non-equilibrium Keldysh formalism. For the elastic regime we show that there is a deep link between the chain conductance and the electrochemical potential drop along the chain. For the inelastic regime we discuss how the quantum interference associated with the electronic transport is damped by the inelastic scattering.

1. Introduction

The transport properties of mesoscopic systems are receiving an increasing amount of attention both experimentally and theoretically (Landauer 1989, Büttiker 1988, Stone and Szafer 1988). These systems are related to different branches of physics like superlattices, heterostructures (Esaki and Tsu 1970), and the scanning tunnelling microscope (Binning *et al* 1982).

Although a great effort has been addressed to the understanding of their elastic conductance only a little work has been done on the effect of inelastic processes (Sols 1992). Büttiker (1989) has proposed a generalization of Landauer's approach to the conductance by including inelastic scattering modelled by electron reservoirs coupled to the wire; this approach has been used by other workers (D'Amato and Pastawsky 1990a, b) to obtain the general properties of the inelastic effects. Other workers have followed a more basic method that is capable of calculating the transport properties of mesoscopic systems from a fundamental point of view (Datta 1990, Anda and Flores 1991).

Even for the case of elastic conductance one- and two-dimensional systems are studied under restricted conditions by assuming a given external potential along the structure; self-consistency between this potential and the induced electronic charge is not usually introduced for obvious reasons: the long computer time one would have to spend on the calculations. In some cases this self-consistency is, however, an essential point; this is the case for a large bias or if we are interested in the electrochemical potential variations along the mesoscopic system (Pernas *et al* 1990, Pernas and Flores 1991).

In this paper we shall analyse the conductance properties of a one-dimensional chain joining two reservoirs, for elastic and inelastic transport regimes. As regards

0953-8984/92/235309+18$04.50

the elastic regime we shall analyse it by introducing a full consistency between the potential acting on the electrons and the charge induced along the chain: the chain conductance, the electrochemical potential variation along the chain and the effect of local defects will be discussed. The inelastic regime will be analysed in the limit of a very small external bias; our specific calculations will show how quantum mechanical fluctuations in the differential conductance dissappear with the inelastic scattering.

In our approach to the previous problems we shall follow the thermodynamical non-equilibrium formalism derived by Keldysh (1964), and developed later by Caroli *et al* (1971). This method affords a fundamental approach to the transport problems (Rammer and Smith 1986). Some people have applied these techniques to the analysis of mesoscopic systems (McLennan *et al* 1991); in general its advantage is that its implementation requires the calculation of only one-particle Green functions, providing all the tools to obtain in a self-consistent way the potential profile created by the external bias. Moreover, the method allows an appropriate description of many-particle effects that can be calculated in principle by introducing the appropriate self-energies, as in causal many-body techniques.

The paper is organized as follows: in section 2 we present our model and the general Keldysh formalism used to solve it. In section 3 we present our results for the elastic system, in section 4 we discuss the inelastic effects in the differential conductance, and section 5 is devoted to conclusions and final remarks.

2. Model and general formalism

Figure 1 shows the model to analyse: a linear chain with n sites is intercalated between two Bethe lattices that play the role of two reservoirs (Pernas *et al* 1990) having chemical potentials μ_L and μ_R (notice that these chemical potentials are only well defined at $-\infty$ and ∞, respectively). The aim of the following analysis is to obtain the conductance properties of the chain for an applied bias, $V = \mu_R - \mu_L$. We describe the elastic properties of the system by means of the following Hamiltonian:

$$\hat{H}_0 = \hat{H}_{\text{Bethe,left}} + \hat{H}_{\text{Bethe,right}} + \sum_{i=1}^{n} E_i \hat{n}_i + \sum_{\sigma;i\neq j} t_{i,j}(\hat{c}^{\dagger}_{i,\sigma}\hat{c}_{j,\sigma} + \hat{c}^{\dagger}_{j,\sigma}\hat{c}_{i,\sigma})$$
$$+ t_{0,1}(\hat{c}^{\dagger}_{0,\sigma}\hat{c}_{1,\sigma} + \hat{c}^{\dagger}_{1,\sigma}\hat{c}_{0,\sigma}) + t_{n,n+1}(\hat{c}^{\dagger}_{n,\sigma}\hat{c}_{n+1,\sigma} + \hat{c}^{\dagger}_{n+1,\sigma}\hat{c}_{n,\sigma}) \quad (1)$$

where E_i represents the diagonal level of the single orbital of each chain site, which could depend upon site i for an applied bias, $t_{i,j}$ the hopping parameter between nearest neighbours in the chain, $t_{0,1}$ and $t_{n,n+1}$ the hopping parameters linking the linear chain to the Bethe lattices, and $\hat{H}_{\text{Bethe}}$ the Hamiltonian of each z-fold coordinated Bethe lattice:

$$\hat{H}_{\text{Bethe}} = \sum_{\sigma;j=1}^{n} E_j \hat{n}_{j,\sigma} + \sum_{\sigma;l\neq p} t_{l,p}(\hat{c}^{\dagger}_{l,\sigma}\hat{c}_{p,\sigma} + \hat{c}^{\dagger}_{p,\sigma}\hat{c}_{l,\sigma}). \quad (2)$$

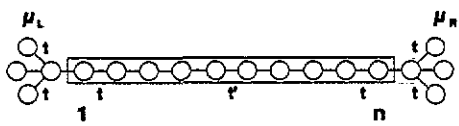

Figure 1. A linear chain with n-sites is joins two Bethe lattice reservoirs.

In general we shall take all the hopping parameters, $t_{i,j}$, $t_{0,1}$ and $t_{n,n+1}$ equal to t_0 except for the central hopping parameter t' shown in figure 1. Defects in the chain will be modelled by taking $t' \neq t$.

Inelastic effects are modelled by on-site electron–electron or electron–phonon interactions, and are assumed to be operative only inside the linear chain. For the electron–electron case we take the following Hamiltonian:

$$\hat{H}_{e-e} = \sum_{i=1}^{n} U \hat{n}_{i,\uparrow} \hat{n}_{i,\downarrow} \tag{3a}$$

while for the electron-phonon case we write

$$\hat{H}_{e-ph} = g^{1/2} \omega_0 \sum_{\sigma;i=1}^{n} \hat{n}_{i,\sigma} (\hat{b}_i^{\dagger} + \hat{b}_i) \tag{3b}$$

where $\hat{b}_i^{\dagger}$ and $\hat{b}_i$ are the creation and annihilation operators associated with the optical phonon of a constant frequency ω_0 localized at the site i, g measuring the electron–phonon coupling.

The chain conductance properties are obtained for a given bias V by using the Keldysh (1964) method that will be summarized below. In this approach the usual retarded and advanced Green functions, $\hat{G}^{R}$ and $\hat{G}^{A}$ respectively, are introduced as well as the non-equilibrium ones, $\hat{G}^{+-}$ and $\hat{G}^{-+}$, defined (Keldysh 1964) by the equations:

$$\hat{G}_{i,j}^{+-}(\omega) = -\mathrm{i}\langle \hat{c}_i \hat{c}_j^{\dagger} \rangle \qquad \hat{G}_{i,j}^{-+}(\omega) = \mathrm{i}\langle \hat{c}_i^{\dagger} \hat{c}_j \rangle \tag{4}$$

where $\langle\ \rangle$ represents mean values taken on the non-equilibrium state of the system; for simplicity we eliminate from now on the spin quantum number σ.

These Green functions are straightfowardly related to the non-equilibrium occupation of the density of states, while $\hat{G}^{R}$ and $\hat{G}^{A}$ only yield the total density of states, irrespective of their occupation. The density of states and the occupation spectra, as well as the density currents, are obtained from $\hat{G}^{R}$, $\hat{G}^{A}$, $\hat{G}^{+-}$ and $\hat{G}^{-+}$. In particular, we should mention that the total current intensity along the linear chain is given by the following (Caroli *et al* 1971) equation:

$$I = \frac{2e}{h} t_0 \int_{-\infty}^{\infty} \mathrm{d}\omega \, [G_{0,1}^{+-}(\omega) - G_{1,0}^{+-}(\omega)]. \tag{5}$$

Equation (5) yields the total current crossing the interface between atoms 0 and 1 as shown in figure 1; obviously, other chain atoms, say i and $i+1$, might have been used to calculate I, but for our purposes this turns out to be the most convenient choice.

It is worth mentioning that equation (5) can be written in a more convenient way as follows (Caroli *et al* 1971):

$$I = \frac{2e}{h} t_0 \int_{-\infty}^{\infty} \mathrm{d}\omega \, [G_{1,1}^{+-}(\omega) g_{0,0}^{-+}(\omega) - G_{1,1}^{-+}(\omega) g_{0,0}^{+-}(\omega)] \tag{6}$$

where the Green functions, $G(\omega)$, have been introduced by taking in our initial Hamiltonian $t_{0,1} = t_{n,n+1} = 0$. In this particular case there is no current intensity

along the linear chain and the different Green function components, $g^{R}_{i,j}$, can be obtained by means of the normal techniques used for equilibrium systems. Thus:

$$g^{+-}_{i,j}(\omega) = 2\,\mathrm{Im}[g^{R}(\omega)][1 - f(\omega)] \qquad g^{-+}_{i,j}(\omega) = -2\,\mathrm{Im}[g^{R}(\omega)]f(\omega)$$

where $f(\omega)$ is the Fermi distribution function. In this paper, we have assumed the temperature to be absolute zero.

In order to calculate $\hat{G}^{+-}$, $\hat{G}^{-+}$, $\hat{G}^{R}$ and $\hat{G}^{A}$ we have used the following Dyson matricial equations:

$$\hat{G}^{R} = \hat{G}^{(0)R} + \hat{G}^{R}\hat{\Sigma}^{R}\hat{G}^{(0)R} \tag{7}$$

$$\hat{G}^{+-} = (\hat{I} + \hat{G}^{R}\hat{\Sigma}^{R})\hat{G}^{(0)+-}(\hat{I} + \hat{\Sigma}^{A}\hat{G}^{A}) + \hat{G}^{R}\hat{\Sigma}^{+-}\hat{G}^{A} \tag{8}$$

where $\hat{G}^{(0)}$ are the undressed Green functions for $\hat{\Sigma} = 0$. In our approach the self-energies, $\hat{\Sigma}^{R}$, $\hat{\Sigma}^{A}$, $\hat{\Sigma}^{+-}$ and $\hat{\Sigma}^{-+}$ only include the many-body effects associated with the electron–electron and the electron–phonon interactions defined by the Hamiltonians (3*a*) and (3*b*); we assume these self-energies to be known, although we discuss this point further below. The Green functions $\hat{G}^{(0)}$ are consequently the solutions of the one-electron Hamiltonian (1), for the applied bias $V = \mu_{R} - \mu_{L}$; they have been calculated using the following Dyson equations:

$$\hat{G}^{(0)R} = \hat{g}^{R} + \hat{G}^{(0)R}\hat{T}\hat{G}^{R} \tag{9}$$

$$\hat{G}^{(0)+-} = (\hat{I} + \hat{G}^{(0)R}\hat{T})\hat{g}^{(0)+-}(\hat{I} + \hat{T}\hat{G}^{A}) \tag{10}$$

where $\hat{T}$ is taken to be the hopping elements between sites 0 and 1, and sites n and $n+1$. In other words, $\hat{T} = 0$ represents the case with the linear chain uncoupled to the Bethe lattices. (Notice that for this one-electron case $\hat{T}^{+-} = 0$; thus, the equivalent of the last term of equation (8) does not appear in equation (10).)

Equations (9) and (10) are the fundamental equations we are going to use in order to analyse the elastic conductance of the chain. In this limit, the many-body effects, measured by the self-energies $\hat{\Sigma}$ in equations (7) and (8) have been neglected. Our elastic limit is not, however, completely determined without a prescription for calculating the potentials induced in the chain and the Bethe lattice sites (E_i and E_j in equations (1) and (2)). We have chosen to relate these potentials to the induced charges at each site, δn_i, by means of the linear equations:

$$\delta V_i = \sum_{j} \alpha_{i,j}\delta n_j \tag{11a}$$

and

$$E_i = E^{(0)} + \delta V_i \tag{11b}$$

where δV_i represents the electrostatic potential induced by the charges, δn_i. Here, δn_i is the induced charge at the site i measured with respect to the case of zero bias. In writing equation (11*b*), we have assumed that all the site levels, E_i and E_j,

are equal to $E^{(0)}$ for zero bias. We should also comment that n_i is given by the following equation

$$n_i = \frac{1}{2\pi i}\int_{-\infty}^{\infty} d\omega\, \hat{G}^{+-}_{i,i}(\omega). \tag{12}$$

The coefficients $\alpha_{i,j}$ are determined by the particular chain geometry. For the sake of simplicity the coefficients $\alpha_{i,j}$ are defined by assuming that there are many linear chains in parallel: then, a site charge is assumed to represent a planar charge extending uniformly in the direction perpendicular to the chain (the planar charge is defined by the surface area per atom, S, we have taken $S = 15$ Å^2; and d, the distance between nearest neighbours, 4 Å). We should comment that this assumption implies large values for the coefficients $\alpha_{i,j}$; then, self-consistency between δV_i and δn_i yields small values of the induced charges, otherwise δV_i would be too large. Our assumptioms for obtaining the coefficients $\alpha_{i,j}$ are not far from local charge neutrality conditions.

The case of inelastic transport is analysed by also considering equations (7) and (8). For this more general case, it is convenient to split G^{+-} (equation (8)) into the elastic and inelastic contributions (Caroli *et al* 1971):

$$\hat{G}^{+-}_{\text{el}} = (\hat{I} + \hat{G}^{\text{R}}\hat{\Sigma}^{\text{R}})\hat{G}^{(0)+-}(\hat{I} + \hat{\Sigma}^{\text{A}}\hat{G}^{\text{A}}) \tag{13a}$$

$$\hat{G}^{+-}_{\text{inel}} = \hat{G}^{\text{R}}\hat{\Sigma}^{+-}\hat{G}^{\text{A}}. \tag{13b}$$

Then, the total current can also be split into its elastic and inelastic parts (Caroli et al 1971): $I = I_{\text{el}} + I_{\text{inel}}$ where

$$I_{\text{el}} = \frac{8e\pi^2 t_0^4}{h}\int_{-\infty}^{\infty} d\omega\, |G^{\text{R}}_{1,n}(\omega)|^2[f_{n+1}(\omega) - f_0(\omega)]\rho_0(\omega)\rho_{n+1}(\omega) \tag{14}$$

$$I_{\text{inel}} = \frac{2e}{h}t_0^4\int_{-\infty}^{\infty} d\omega \sum_{i=1}^{n} |\, G^{\text{R}}_{1,i}(\omega)\,|^2\,[\Sigma^{+-}_{i,i}(\omega)g^{-+}_{0,0}(\omega) - \Sigma^{-+}_{i,i}g^{+-}_{0,0}]. \tag{15}$$

In equation (14) $f_0(\omega)$ and $f_{n+1}(\omega)$ are the Fermi distribution functions for the two reservoirs, and $\rho_0(\omega)$ and $\rho_{n+1}(\omega)$ the local density of states for sites 0 and $n+1$ for the two Bethe lattices, respectively, when they are decoupled from the chain. In obtaining equation (15) we have made a further assumption: we have taken only diagonal self-energy components; in other words, we approximate $\hat{\Sigma}$ by its diagonal components $\Sigma_{i,i}$ and neglect off-diagonal terms, $\Sigma_{i,j}$, if $i \neq j$. Needless to say that only equation (14) should be used for the elastic transport case, with $\hat{G}$ replaced by $\hat{G}^{(0)}$.

The elastic electrical current given by equation (14) depends on the properties of the sites 0 and $n+1$ for equilibrium conditions, and on the $G^{\text{R}}_{1,n}$ Green function which describes how electrons propagate along the chain between sites 1 and n. We should mention that $G^{\text{R}}_{1,n}$ depends on the retarded self-energies, $\Sigma^{\text{R}}_{i,i}$; in this case, these self-energies play the role of an optical potential acting locally on the electron. The inelastic intensity given by equation (13) is, however, directly proportional to the self-energies $\Sigma^{+-}_{i,i}$ and $\Sigma^{-+}_{i,i}$, which yield the way in which the inelastic scattering inside the linear chain induces an inelastic current from site 0 to site 1. It should

be kept in mind, however, that although the total current is independent of the sites used to calculate it (in our case $0 \mapsto 1$), the splitting into the elastic and inelastic currents is not. This is related to the inelastic scattering an electron suffers as it goes along the chain changing its contribution from an elastic to an inelastic current.

Equations (14) and (15) will be used below to calculate the effect of the inelastic scattering on the linear chain conductance. Let us mention now that in obtaining equations (14) and (15), the self-energies $\Sigma^{R}_{i,i}$, $\Sigma^{A}_{i,i}$, $\Sigma^{+-}_{i,i}$ and $\Sigma^{-+}_{i,i}$ have been assumed to be known. A fully consistent solution to the linear chain inelastic conductance can only be obtained by a detailed calculation of the different self-energies; in this paper, instead of doing this calculation, we shall follow a different approach and study the inelastic scattering effects by means of an effective parameter, the quasiparticle lifetime, that yields the main effects associated with the different self-energies. We shall discuss this point in section 4.

3. Elastic conductance

First of all we consider the electrochemical potential variations along different linear chains, changing its length, the mean Fermi energy and the applied bias.

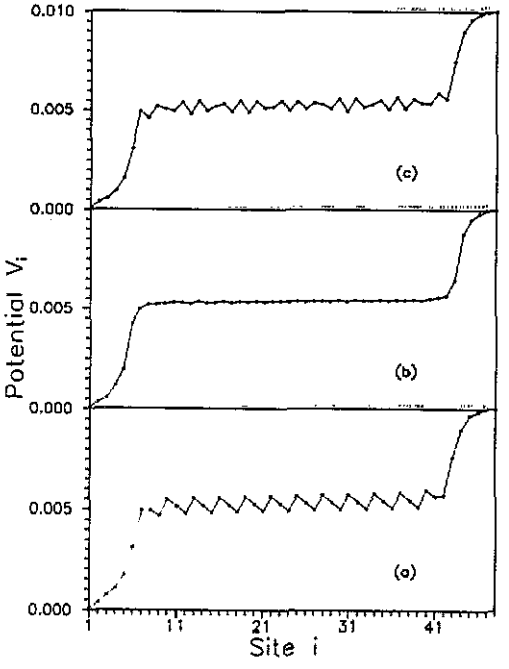

Figure 2. The electrochemical potential variations along the linear chain and the two reservoirs, for: (*a*) $n = 36$, $\mu_L = -1.005$ and $\mu_R = -0.995$ (chain sites 7–42). (*b*) $n = 38$, $\mu_L = -1.005$ and $\mu_R = -0.995$ (chain sites 7–44). (*c*) $n = 38$, $\mu_L = -0.505$ and $\mu_R = -0.495$ (chain sites 7–44). The Bethe lattices extend six sites from each end of the linear chain.

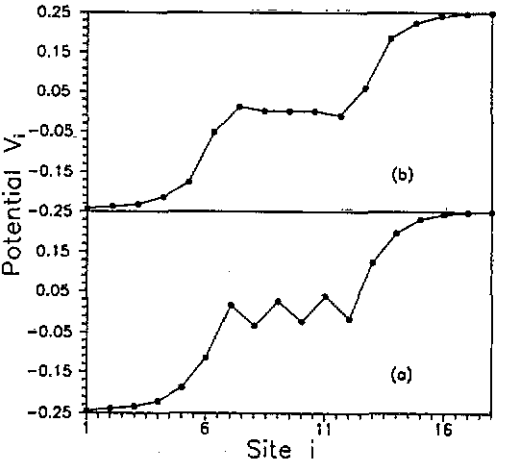

Figure 3. As figure 2 for: (*a*) $n = 6$, $\mu_L = -0.25$ and $\mu_R = 0.25$ (chain sites 7–12); (*b*) $n = 5$, $\mu_L = -0.25$ and $\mu_R = 0.25$ (chain sites 7–11).

Figures 2 and 3 show the electrochemical potential variations along the chain for the following cases

(a) $n = 36, E_i = 0, t = t' = 1, \mu_L = -1.005$ and $\mu_R = -0.995$
(b) $n = 38, E_i = 0, t = t' = 1, \mu_L = -1.005$ and $\mu_R = -0.995$
(c) $n = 38, E_i = 0, t = t' = 1, \mu_L = -0.505$ and $\mu_R = -0.495$
(d) $n = 6, E_i = 0, t = t' = 1, \mu_L = -0.250$ and $\mu_R = 0.250$
(e) $n = 5, E_i = 0, t = t' = 1, \mu_L = -0.250$ and $\mu_R = 0.250$.

In all these cases, the applied bias $\mu_R - \mu_L$ is small enough to give a linear response of the system. Cases (d) and (e) (figure 3) have been taken from Pernas *et al* (1990), where the local charge neutrality conditions were used to calculate the electrochemical potential along the chain. It is interesting to see how the potential variations along the chain depend on its length and the mean Fermi energy. First of all it is important to notice that in all the cases studied the applied voltage falls mainly around Bethe lattice contacts of the chain, oscillating around a constant value in the chain. For $n = 36$ and $\frac{1}{2}(\mu_R + \mu_L) = -1$ we find the oscillations in the electrochemical potential shown in figure 2(*a*); these oscillations correspond to the Fermi wavelength appearing at $E_f = -1$ (for this energy, the Fermi wavelength extends three atoms along the linear chain). The main reason for the appearance of these oscillations is the constructive interference between the chain length ($n = 36$) and the Fermi wavelength (three atoms). We have checked this point by changing n from 36 to 38, keeping μ_R and μ_L constant. Figure 2(*b*) shows the electrochemical potential variations along the chain: because of the lack of constructive interference between the chain length and the Fermi wavelength ($n = 38$ is not a multiple of this length), we find that the potential is constant along the chain. In a further step, we have changed $\frac{1}{2}\mu_R + \mu_L$ from -1 to -0.5, keeping $n = 36$; for this case, we find the solution shown in figure 2(*c*), with local fluctuations having no regular pattern. For this case, the chain length is not a multiple of the Fermi wavelength, which is 2.38 atoms; the electrochemical potential shown in figure 2(*c*) presents, however, small irregularities in its periodicity, which changes between wavelengths of two and three atoms.

The results of figure 2 show the great importance of having the right interference between the chain length and the Fermi wavelength, in order to obtain periodic oscillations in the electrochemical potential profile along the chain. Similar results were obtained in Pernas *et al* (1990) for shorter chains; for the sake of completeness we reproduce here, in figure 3, the results calculated by Pernas *et al* (1990) for the chains of length $n = 6$ and 5. For the case $n = 6$ and $\frac{1}{2}\mu_R + \mu_L = 0$ the chain length is a multiple of the Fermi wavelength (two atoms) and the electrochemical potential shows the oscillations of figure 3(*a*). For the case $n = 5$ and $\frac{1}{2}\mu_R + \mu L = 0$, the chain length and the Fermi wavelength do not interfere constructively, yielding the constant potential shown in figure 3(*b*). Previous results have been obtained for a small bias, within a linear-response regime. In order to explore the effect of larger biases, we have analysed the case $n = 30$, with $\frac{1}{2}\mu_R + \mu_L = -1$ and different values of $\mu_R - \mu_L = 0.1, 0.2, 0.3, 0.4, \ldots, 0.9$ and 1. Figure 4 shows the results we have obtained for the electrochemical potential along the chain. It is worth realizing that for $\mu_R - \mu_L = 0.1$ and 0.2, we are close to the linear response regime. Morover, for this case $n = 30$ is a multiple of the Fermi wavelength, and the potential shows the periodicity associated with this length (three atoms). For $\mu_R - \mu_L > 0.3$ we find a non-linear regime with the potential profile changing with respect to the linear

case. These changes are more important for larger applied biases and, eventually, for $\mu_R - \mu_L \geqslant 0.5$, the regular periodicity of the potential profile is lost: this is obviously because the wavelength of the new electrons contributes to the elastic current. Increasing the bias we find new electrons with different wavelengths; this effect destroys the coherence between the chain length and the wavelength of the electrons contributing to the current.

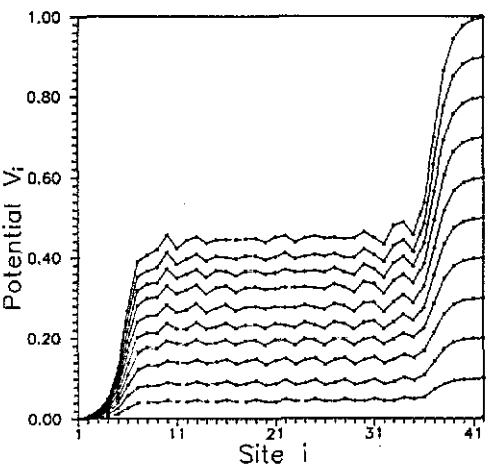

Figure 4. Electrochemical potential variations along the linear chain for $n = 30$, $\frac{1}{2}(\mu_L + \mu_R) = -1$ and different values of $\mu_R - \mu_L$ (0.1,0.2,0.3,...,0.9 and 1.0) (chain sites 7–36).

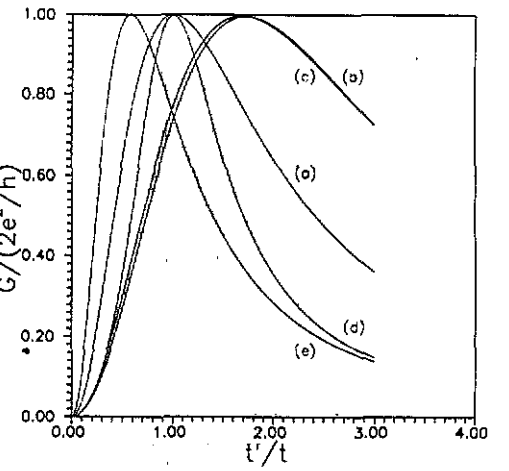

Figure 5. Conductance of a linear chain in units of $2e^2/h$ as a function of t'/t for: (*a*) $n = 38$, $\frac{1}{2}(\mu_R + \mu_L) = -1$; (*b*) $n = 36$, $\frac{1}{2}(\mu_R + \mu_L) = -1$; (*c*) $n = 38$, $\frac{1}{2}(\mu_R + \mu_L) = -0.5$; (*d*) $n = 5$, $\frac{1}{2}(\mu_R + \mu_L) = 0$; (*e*) $n = 6$, $\frac{1}{2}(\mu_R + \mu_L) = 0$.

Let us turn our attention to analysing the conductance of the linear chain. We shall present our results by considering the case $t' \neq t$; this implies assuming to have a defect at the centre of the linear chain (see figure 1). First of all, we are going to analyse the conductance, G, of differents chains for a small applied bias ($\mu_R - \mu_L$ is assumed to be very small) as a function of t'/t. Figure 5, shows $G = I/(\mu_R - \mu_L)$ as a function of t'/t for the following cases: (a), $n = 38$, $\frac{1}{2}\mu_R + \mu_L = -1$; (b), $n = 36$, $\frac{1}{2}\mu_R + \mu_L = -1$; (c), $n = 38$, $\frac{1}{2}\mu_R + \mu_L = -0.5$; (d), $n = 5$, $\frac{1}{2}\mu_R + \mu_L = 0$; (e), $n = 6$ and, $\frac{1}{2}\mu_R + \mu_L = 0$, in correspondence with the cases discussed above. The results of figure 5 show a maximum, $2e^2/h$, for the conductance in all the cases: this is obviously the maximum value a one-dimensional chain can have. This maximum appears, however, for the different cases at different values of t'/t. What is of interest to realize is that this maximum appears for $t'/t = 1$ for cases (a) and (d) only; it should be remembered that in these particular cases the electrochemical potential is constant along the chain. In the other cases the conductance maximum appears for values of t'/t close to 0.58 or 1.71. These results show that the potential oscillates along the chain if the conductance is smaller than $2e^2/h$.

We also explored the elastic conductance of the chain as a function of the Fermi level, for $t'/t = 1$. Using the Keldysh method discussed above, we have obtained the following analytical value:

$$G = (2e^2/h)4c^2 \sin^2 \alpha \sin^2 \alpha'/(4c^2 \sin^2 \alpha \sin^2 \alpha' + A^2) \qquad (16a)$$

where

$$A = \sin[(n+1)\alpha] + c^2 \sin[(n-1)\alpha] + 2c \cos \alpha' \sin n\alpha \qquad (16b)$$

and

$$\cos \alpha' = -(cE_f/2t) \qquad \cos \alpha = -(E_f/2t) \qquad c = 1/(z-1)^{1/2}. \qquad (16c)$$

Here E_f is the Fermi level referred to the centre of the band and z is the coordination number of the Bethe lattice (taken to be four in this paper). Equation (16*a*) shows that the maximum of G, $2e^2/h$, appears for $A = 0$; this condition expresses the lack of interference between the Fermi wavelength and the chain length, as discussed above. Figure 6 shows this linear conductance for $n = 36$ and 38; notice the oscillations appearing in the conductance, and that G has a maximum for $n = 38$ and $E_f = -1$, while a minimum appears close to the other cases discussed above ($n = 38, E_f = -0.5$; $n = 36, E_f = 0$; $n = 36, E_f = -1$). In general, a maximum in the conductance as a function of E_f, implies no voltage drop along the chain while, for a minimum, regular oscillations in the electrochemical potential appear along the chain.

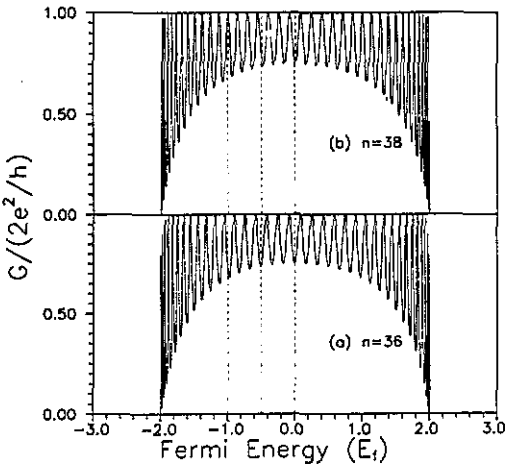

Figure 6. Linear conductance, in units of $2e^2/h$, as a function of the Fermi level, referred to the middle of the conduction band, for: (*a*) $n = 36$; (*b*) $n = 38$.

It is worth commenting that by starting with one of the cases where the conductance has a minimum as a function of E_f (say, $n = 38, E_f = 0$, and $t'/t = 1$) one can increase G by changing t'/t appropriately. Then a maximum in the conductance appears taking for t'/t the values $(z-1)^{1/2}$ or $1/(z-1)^{1/2}$ (as found above in figure 5 for $z = 4$), depending on the length of the chain and the order of the oscillations associated with the conductance maximum (for the sake of brevity we do not discuss these results in more detail).

We have also analysed the potential variations along the chain for values of t'/t close to the one in which the conductance has a maximum. We have chosen the case $n = 38$, $E_f = -0.5$ and t'/t close to 1.71. Figure 7 shows our results for t'/t equal to 1.2, 1.65 and 1.8. This figure shows that the potential has a small drop across the chain defect, for t'/t larger or smaller than 1.65. Notice that this drop changes its sign when t'/t crosses the value 1.65.

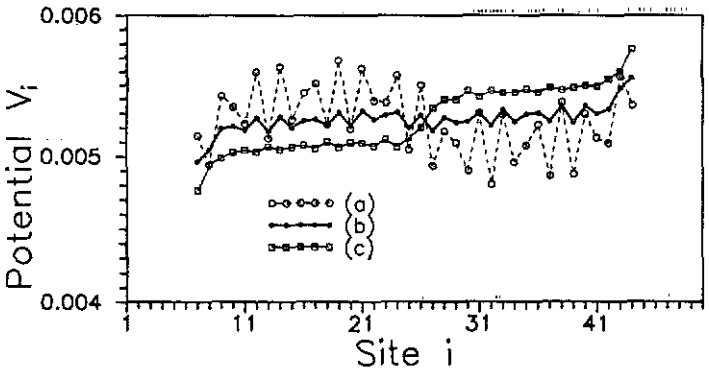

Figure 7. Electrochemical potential variations along the chain for $n = 38$, $\frac{1}{2}(\mu_R + \mu_L) = -0.5$ and different values of t'/t: (*a*) $t'/t = 1.2$; (*b*) $t'/t = 1.65$; (*c*) $t'/t = 1.8$.

We have also analysed the non-linear conductance of a linear chain in order to see how saturation effects in the current appear for high applied biases. Figure 8 shows $G = I/(\mu_R - \mu_L)$, for $n = 38$, $\frac{1}{2}(\mu_R + \mu_L) = -0.5$, and $\mu_R - \mu_L = 0.01, 0.1, 0.5$ and 2, as a function of t'/t. The case $\mu_R - \mu_L = 0.01$ represents a linear transport regime with $G_{max} = 2e^2/h$, while for larger bias the maximum conductance is lower than $2e^2/h$. Moreover, for the non-linear cases the maximum of the conductance tends to appear around $t'/t = 1$, at variance with the linear regime. Let us remark, finally, that the maximum conductance decreases with increasing values of $\mu_R - \mu_L$ (increasing non-linearity).

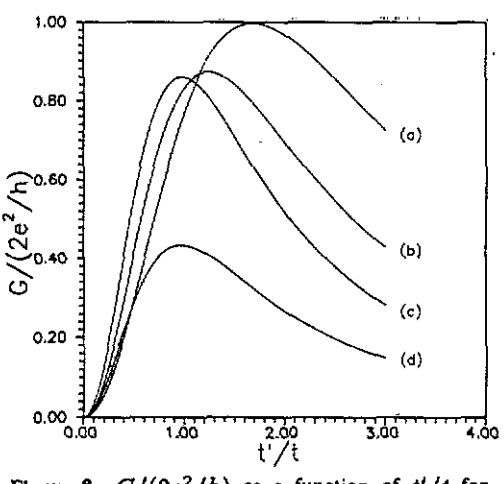

Figure 8. $G/(2e^2/h)$ as a function of t'/t for $n = 38$, $\mu_R + \mu_L = -0.5$ and different values of $\mu_R - \mu_L$: (*a*) 0.01; (*b*) 0.1; (*c*) 0.5; (*d*) 2.0.

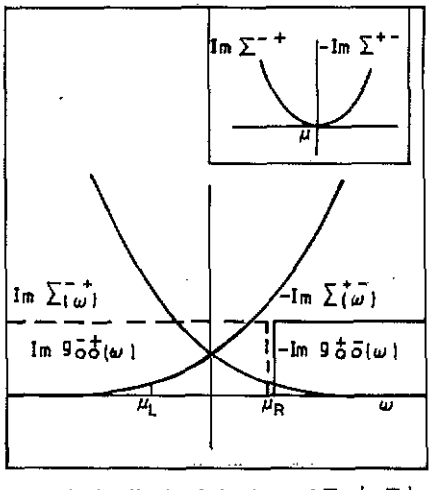

Figure 9. Qualitative behaviour of Σ^{-+}, Σ^{+-} and $g^{+-}_{0,0}$ as functions of ω. The inset shows Σ^{-+} and Σ^{+-} for the equilibrium case, $\mu_L = \mu_R = \mu$.

4. Inelastic conductance

We have analysed how inelastic effects modify the chain conductance in the limit of very small bias, the case of the linear regime. At the same time we are going to assume that the electron inelastic mean free path, λ, is much larger that the chain length, L. A more general case will be discussed qualitatively in the next section.

In the limit $\lambda \gg L$ we expect that the inelastic effects do not change appreciably the elastic solution calculated in the previous section. Now, we shall proceed to calculate the lowest order effects introduced by the inelastic scattering.

In this paper we shall discuss specifically the electron–electron interaction (equation (3*a*)) effects on the conductance. As mentioned above we shall use a local approximation to calculate $\hat{\Sigma}$; a second order perturbative calculation in U yields the lowest inelastic contribution to $\hat{\Sigma}_{i,i}$:

$$\Sigma^{-+}_{i,i} = \frac{U^2}{(2\pi)^2}\int_{-\infty}^{\infty} dE_2\, dE_3\, dE_4\, G^{(0)+-}_{i,i}(E_2)G^{(0)-+}_{i,i}(E_3)G^{(0)-+}_{i,i}(E_4) \times \delta(\omega + E_2 - E_3 - E_4) \tag{17}$$

with a similar equation for $\Sigma^{+-}_{i,i}$. Here $\hat{G}^{(0)}$ is the elastic Green function ($\hat{\Sigma} = 0$). In the inset of figure 9 we show the qualitative behaviour of $\hat{\Sigma}^{+-}$ and $\hat{\Sigma}^{+-}$ as given by equation (17) for a zero applied bias ($\mu = \mu_R = \mu_L$). In this case, $\hat{\Sigma}^{+-} = 0$ for $\omega < \mu$, while $\hat{\Sigma}^{-+} = 0$ for $\omega > \mu$ ($\hat{\Sigma}^{+-}$ and $\hat{\Sigma}^{-+}$ are purely imaginary quantities); both self-energies tend to zero, for ω going to μ, like $(\omega - \mu)^2$. We should mention that in general:

$$2\,\mathrm{Im}[\Sigma^R(\omega)] = \Sigma^{+-}(\omega) - \Sigma^{-+}(\omega) \tag{18}$$

in such a way that the inset of figure 9 yields around $\mu = \mu_R = \mu_L$, the well known behaviour for $\mathrm{Im}\Sigma^R$ when one considers the Hamiltonian 3(*a*).

For $\mu_R \neq \mu_L$ we can expect that the induced currents around the Fermi energy broaden Σ^{+-} and Σ^{-+}, as shown in figure 9 (the results of this figure have been obtained by assuming that the electron states between μ_R and μ_L are half-occupied). As shown in figure 9 Σ^{+-} and Σ^{-+} are mirror images of each other with respect to $\frac{1}{2}(\mu_R + \mu_L)$, for small values of $\omega - \frac{1}{2}(\mu_R + \mu_L)$. This symmetry is a consequence of the symmetrical electronic excitations appearing around $\frac{1}{2}(\mu_R + \mu_L)$ arising from the currents induced along the chain. Let us mention at this point that, in a perfect one-dimensional chain without defects, the forward and backward induced elastic currents should be the same at all the atoms of the chain. On the other hand, if the chain is long enough, with $n \gg 1$, the local density of states at each atom is the same except for the few atoms around the contacts. Then, we can expect $\Sigma_{i,i}$ to be the same for almost all the chain sites. For $n \gg 1$ we shall take from now on:

$$\Sigma_{i,i}(\omega) = \Sigma(\omega) \tag{19}$$

and obtain all the inelastic effects using this equation with $\hat{\Sigma}$ calculated for the atoms located well inside the chain. Let us stress that this is only a valid approximation in the limit $n \gg 1$, a case for which the contact effects between the linear chain and the reservoirs can be neglected.

The inelastic current given by equation (15) now takes the form:

$$I_{\text{inel}} = \frac{2e}{h}t_0^2 \int_{-\infty}^{\infty} d\omega\,[\Sigma^{+-}(\omega)g_{0,0}^{-+}(\omega) - \Sigma^{-+}(\omega)g_{0,0}^{+-}(\omega)] \sum_{i=1}^{n} |\, G_{1,i}^{(0)R}(\omega)\,|^2 \qquad (20)$$

to first order in the inelastic scattering. In figure 9 we also show $g_{0,0}^{-+}(\omega)$ and $g_{0,0}^{+-}(\omega)$; according with the definition given above, we can write:

$$g_{0,0}^{+-}(\omega) = -2\pi i\rho_0(\omega)[1 - f_L(\omega)] \qquad (21a)$$

$$g_{0,0}^{-+}(\omega) = 2\pi i\rho_0(\omega)f_L(\omega) \qquad (21b)$$

where $\rho_0(\omega)$ is the local density of states in the 0-site for the uncoupled Bethe lattice and $f_L(\omega)$ the Fermi distribution function for $\mu = \mu_L$. Thus, $g_{0,0}^{+-}(\omega)$ ($g_{0,0}^{-+}(\omega)$) is different from zero only for ω larger (smaller) than μ_L.

Figure 9 and equations (21) show that the factor

$$\int_{-\infty}^{\infty} d\omega\,[\Sigma^{+-}(\omega)g_{0,0}^{-+}(\omega) - \Sigma^{-+}(\omega)g_{0,0}^{+-}(\omega)]$$

inside equation (20) can be replaced, for a small bias, by

$$\pi\rho_0(\mu_0)(\mu_R - \mu_L)\text{Im}[\langle(\Sigma^{+-} - \Sigma^{-+})\rangle]$$

where $\mu_0 = \frac{1}{2}(\mu_R + \mu_L)$ and $\langle\ \rangle$ means an average in the region $\mu_L < \omega < \mu_R$. Using equation (18), we can write the inelastic current as follows:

$$I_{\text{inel}} = \frac{4e}{h}t_0^2\rho_0(\mu_0)\text{Im}\langle\Sigma^R\rangle(\mu_R - \mu_L)\sum_{i=1}^{n} |\, G_{1,i}^{(0)R}(\mu_0)\,|^2\,. \qquad (22)$$

Let us also mention that the elastic current, I_{el}, should be calculated with equation (14), using the full Green function, $G_{1,n}^R(\omega)$, instead of the elastic one, $G_{1,n}^{(0)R}(\omega)$. This implies that the inelastic scattering contributes to the elastic component of the current through the modification of the retarded Green function, $\hat{G}^R$. Notice that $\hat{G}^R$ satisfies the following equation:

$$\hat{G}^R = \hat{g}^R + \hat{G}^R(\hat{T} + \Sigma^R)\hat{g}^R \qquad (23)$$

as can be found by combining equations (7) and (9).

$\hat{G}^R$ will be calculated in first order with respect to $\hat{\Sigma}^R$, and then introduced in equation (4). This yields

$$I_{el} = (8e\pi^2/h)t_0^4(\mu_R - \mu_L)\rho_0(\mu_0)\rho_{n+1}(\mu_0)\,|\,\langle G_{1,n}^R(\mu_0)\rangle\,|^2$$

where $\langle G_{1,n}^R(\mu_0)\rangle$ is the Green function $G_{1,n}^R(\omega)$, as calculated from equation (23), replacing ω by the mean Fermi energy, μ_0, and Σ^R by its mean value $\langle\Sigma^R\rangle$ in the interval $\mu_L < \omega < \mu_R$. $\langle G_{1,n}^R(\mu_0)\rangle$ depends, accordingly, on the real and the imaginary components of $\langle\Sigma^R\rangle$. The effect of $\text{Re}\langle\Sigma^R\rangle$ on the inelastic transport is to introduce a phaseshift in the different physical magnitudes of the problem,

while $\mathrm{Im}\langle\Sigma^{\mathrm{R}}\rangle$ yields a damping effect typical of all inelastic processes. For instance, $\mathrm{Re}\langle\Sigma^{\mathrm{R}}\rangle$ can change the phaseshift of the electrochemical potential variation along the chain, and modify the interference between the Fermi wavelength and the chain length. We shall concentrate, however, on discussing how $\mathrm{Im}\langle\Sigma^{\mathrm{R}}\rangle$ affects the current and damps some of the oscillations appearing in the conductance as a function of the Fermi level (figure 6); this implies that our results are going to depend only on the quantity $\mathrm{Im}\langle\Sigma^{\mathrm{R}}\rangle$, which is going to mesure how inelastic effects modify the current with respect to the elastic regime.

Equations (24) and (22) yield the elastic and inelastic components of the total current as functions of the Green functions $\hat{G}^{(0)\mathrm{R}}$ and $\hat{G}^{\mathrm{R}}$, given by equations (9) and (23), respectively.

Without going into more details we write down the elastic and inelastic components of the total current as calculated from those equations. The elastic component is given by

$$G_{\mathrm{el}} = I_{\mathrm{el}}/(\mu_{\mathrm{R}} - \mu_{\mathrm{L}}) = (2e^2/h)4c^2 \sin^2\alpha \sin^2\alpha'/(4c^2 \sin^2\alpha \sin^2\alpha' + A^2 + \Delta) \tag{25a}$$

where A, α, α' and c have been defined above, and

$$\Delta = -n(\mathrm{Im}\langle\Sigma^{\mathrm{R}}\rangle/t_0 \sin\alpha)[2c(1+c^2)\sin\alpha \sin\alpha' + c^2 \sin 2\alpha \sin 2\alpha']. \tag{25b}$$

Notice that Δ yields how inelastic processes affect the elastic current. As mentioned above this is owing to the 'optical potential' created by the electron self-energy.

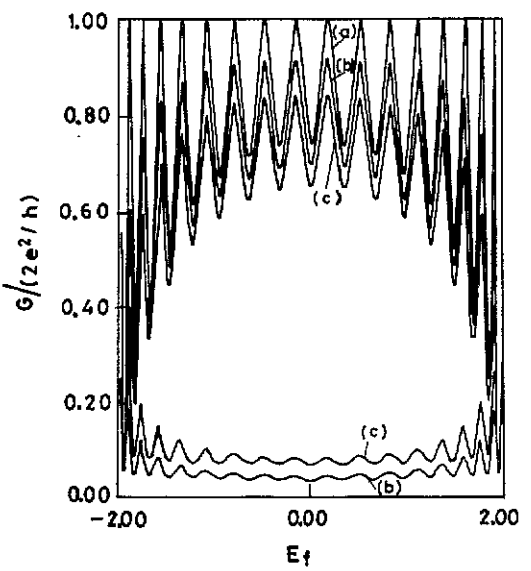

Figure 10. Linear conductance, $G/(2e^2/h)$, as a function of the Fermi level for $n = 16$ and: (*a*) $\mathrm{Im}\langle\Sigma^{\mathrm{R}}\rangle = 0$; (*b*) $\mathrm{Im}\langle\Sigma^{\mathrm{R}}\rangle = 0.004t$ and (*c*) $\mathrm{Im}\langle\Sigma^{\mathrm{R}}\rangle = 0.008t$. In cases (*b*) and (*c*) we show the elastic and inelastic conductances; the inelastic contribution being the smallest one.

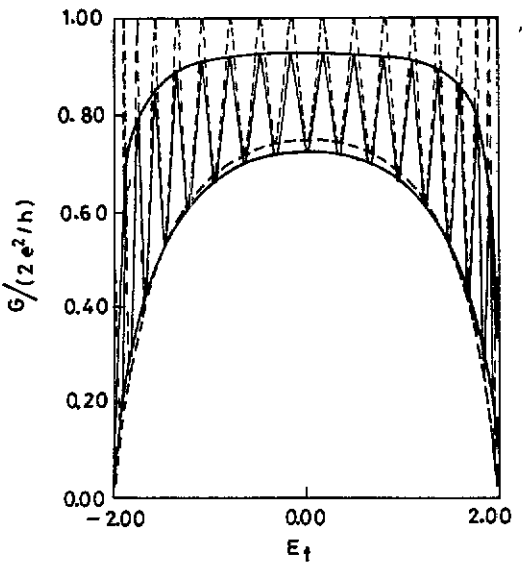

Figure 11. Linear conductance, $G/(2e^2/h)$, as a function of the Fermi level for $n = 16$. This figure includes the elastic and the inelastic contributions for $\mathrm{Im}\langle\Sigma^{\mathrm{R}}\rangle = 0.008t$. The broken curve corresponds to $\mathrm{Im}\langle\Sigma^{\mathrm{R}}\rangle = 0$.

Equation (25*a*) yields for $\Delta = 0$ the solution given in equation (16*a*). Figure 10 shows this elastic solution for $n = 16$ as a function of the Fermi energy; the elastic conductance for $\Delta = 0$ behaves like those presented in figure 6 for $n = 36$ and 38. In order to discuss how the inelastic processes affect the conductance, it is convenient to calculate the maximum and minimum envelopes of the elastic current (with $\Delta = 0$). From equations (16) we obtain

$$G_{el}^{max}(\Delta = 0) = 2e^2/h \tag{26a}$$

and

$$G_{el}^{min}(\Delta = 0) = (2e^2/h)4c^2 \sin^2 \alpha \sin^2 \alpha' \{4c^2 \sin^2 \alpha \sin^2 \alpha' + [(1 + c^2)\cos \alpha + 2c \cos \alpha]^2 + (1 - c^2)^2 \sin^2 \alpha\}^{-1}. \tag{26b}$$

Equation (26*a*) is obtained by taking $A = 0$ in equation (16*a*), while equation (26*b*) is obtained by calculating the maximum of A in the same equation (16*a*).

The elastic contribution to the total current, for the inelastic regime, can also be analysed in the same way. From equations (25), we get that the maximum and the minimum envelopes of $G_{el}(\Delta \neq 0)$ are given by

$$G_{el}^{max}(\Delta \neq 0) = (2e^2/h)4c^2 \sin^2 \alpha \sin^2 \alpha'/(4c^2 \sin^2 \alpha \sin^2 \alpha' + \Delta) \tag{27a}$$

$$G_{el}^{min}(\Delta \neq 0) = (2e^2/h)4c^2 \sin^2 \alpha \sin^2 \alpha' \{4c^2 \sin^2 \alpha \sin^2 \alpha' + [(1 + c^2)\cos \alpha + 2c \cos \alpha]^2 + (1 - c^2)^2 \sin^2 \alpha + \Delta\}^{-1}. \tag{27b}$$

We should mention at this point that Δ is always positive, because $\mathrm{Im}\langle \Sigma^R \rangle$ is negative. Then $G_{el}^{max}(\Delta \neq 0)$ is always smaller than $2e^2/h$, and $G_{el}^{min}(\Delta \neq 0)$ is also smaller than $G_{el}^{min}(\Delta = 0)$. Figure 10 shows how G_{el}^{max} and G_{el}^{min} depend on Δ, for $n = 16$. As this figure shows, an increase in Δ reduces the elastic contribution to the current and its oscillations as a function of the Fermi energy. Notice that these envelope functions depend only on $\mathrm{Im}\langle \Sigma^R \rangle$ but not on $\mathrm{Re}\langle \Sigma^R \rangle$; this real part of $\langle \hat{\Sigma} \rangle$ would only modify the relative position of the conductance oscillations.

As regards the inelastic contribution to the total current we find the following equation:

$$G_{inel} = \frac{I_{inel}}{\mu_R - \mu_L} = -\frac{2e^2}{h} \frac{n\,\mathrm{Im}\langle \Sigma^R \rangle \sin \alpha \sin \alpha' (1 + c^2 + 2c \cos \alpha \cos \alpha')}{t_0 \sin \alpha \qquad 4c^2 \sin^2 \alpha \sin^2 \alpha' + A^2}. \tag{28}$$

The maximum and the minimum envelopes of G_{inel} are given by

$$G_{inel}^{max} = -\frac{2e^2}{h} \frac{n\,\mathrm{Im}\langle \Sigma^R \rangle}{t_0 \sin \alpha} \frac{(1 + c^2 + 2c \cos \alpha \cos \alpha')}{4c^2 \sin \alpha \sin \alpha'} \tag{29a}$$

$$G_{inel}^{min} = -\frac{2e^2}{h} \frac{n\,\mathrm{Im}\langle \Sigma^R \rangle}{t_0 \sin \alpha} \sin \alpha \sin \alpha' (1 + c^2 + 2c \cos \alpha \cos \alpha') \{4c^2 \sin^2 \alpha \sin^2 \alpha' + [(1 + c^2)\cos \alpha + 2c \cos \alpha']^2 + (1 - c^2)\sin^2 \alpha\}^{-1}. \tag{29b}$$

Contrary to what happens with the elastic current the inelastic contribution and its oscillations increase with $\mathrm{Im}\langle \Sigma^R \rangle$. The behaviour of both the elastic and the inelastic components to the current are shown in figure 10, for $n = 16$.

In order to see how the envelop of the maximum of the total current changes with $\mathrm{Im}\langle\Sigma^{\mathrm{R}}\rangle$ it is convenient to combine equations (27*a*) and (27*b*) From these equations we find that the effect of $\mathrm{Im}\langle\Sigma^{\mathrm{R}}\rangle$ is to lower the envelop of the conductance maximum; defining $\delta G^{\max}$ as follows:

$$G_{\mathrm{el}}^{\max} + G_{\mathrm{inel}}^{\max} = 2e^2/h + \delta G^{\max} \tag{30}$$

we find, up to first order in $\mathrm{Im}\langle\Sigma^{\mathrm{R}}\rangle$:

$$\delta G^{\max} = \left(\frac{2e^2}{h}\right)\left(\frac{n\,\mathrm{Im}\langle\Sigma^{\mathrm{R}}\rangle}{t_0 \sin\alpha}\right)\frac{(1 + c^2 + 2c\cos\alpha\cos\alpha')}{4c^2\sin\alpha\sin\alpha'} \tag{31}$$

a result consistent with equation (29*a*) since

$$2e^2/h - G_{\mathrm{el}}^{\max} = 2G_{\mathrm{inel}}^{\max} = -2\delta G^{\max}. \tag{32}$$

Equation (32) shows that up to first order in the parameter $\mathrm{Im}\langle\Sigma^{\mathrm{R}}\rangle$, the envelope of the maximum current is lowered as much as the value of the envelope of the maximum inelastic current increases. This is also seen in the results presented in figure 10. We conclude that the inelastic scattering reduces the total current with respect to the elastic case ($\mathrm{Im}\langle\Sigma^{\mathrm{R}}\rangle = 0$). This reduction is shown in figure 11, for $n = 16$.

The lower envelope of the total current can be studied by combining equations (27*b*) and (29*b*). Figure 11 shows how the minima evolve with $\mathrm{Im}\langle\Sigma^{\mathrm{R}}\rangle$. The envelopes are shown in figure 11 as a function of the Fermi level that is assumed to move across the one-dimensional chain band width. The main point to notice about this figure is how the total conductance and its oscillations are reduced for increasing values of $\mathrm{Im}\langle\Sigma^{\mathrm{R}}\rangle$.

It is worthwhile mentioning that although for reasons of exposition we have presented in figures 10 and 11 the transport properties of the linear chain as a function of $\mathrm{Im}\langle\Sigma^{\mathrm{R}}\rangle$, what really matters for the definition of the lower and upper envelopes and, as a consequence, for the oscillation amplitudes, is the product $n\,\mathrm{Im}\langle\Sigma^{\mathrm{R}}\rangle$. This is evident from the inspection of equations (25*b*) and (29).

The inelastic processes reduce the total current as they reduce the drift velocity of the carriers. Simultaneously they introduce a mechanism through which the electron loses the memory of its phase at a distance of the order of the mean free path (Altshuler *et al* 1982). Although we are in a region where the sample length is much shorter than the mean free path, this lose of memory reflects itsef in the fact that the current oscillations, as a function of the Fermi level, are reduced in amplitude owing to a reduction of quantum interference as the inelastic scattering parameter $\mathrm{Im}\langle\Sigma^{\mathrm{R}}\rangle$ increases.

5. Discussion and concluding remarks

In this paper we have analysed the transport properties of a one-dimensional chain joining two reservoirs. The chain conductance, the electrochemical potential variations along the chain and other related properties have been discussed, keeping in mind the understanding of how the chain properties are related to the quantum mechanical interference effects appearing between the electron and the chain length.

First of all, we have discussed the elastic regime: in this case, electrons move elastically from one reservoir to the other, or are assumed to be scattered by a localized defect. Our analysis shows that there is a deep link between the chain conductance and the electrochemical potential variations along the chain. The conductance of an ideal chain as a function of its mean Fermi energy has oscillations with different maximum values of $2e^2/h$. For these maxima, the electrochemical potential is constant along the chain. For the minimum in the conductance as a function of the Fermi energy, the electrochemical potential shows, however, oscillations that are related to the electron Fermi wavelength: the conductance minimum is the result of a constructive interference for the electrochemical potential between that Fermi wavelength and the chain length. It is also of interest to notice that for these cases (conductance minimum), a chain defect can destroy the above mentioned constructive interference and modify the chain conductance: we have also found that by appropriately choosing the scattering properties of the defect one can obtain a maximum in the chain conductance (the defect introduces the appropriate destructive interference between the Fermi electron wavelength and the chain length, in order to maximize the chain conductance).

Nonlinear effects for the elastic regime have also been discussed. In general, we find that non-linear effects reduce the chain conductance, introducing large fluctuations in the electrochemical potential variations along the chain.

The inelastic regime has also been analysed in this paper. In this case we have only discussed how inelastic processes modify the oscillations appearing in the conductance of an ideal chain as a function of the mean Fermi energy. One can think, extrapolating the results obtained for the elastic case, that these modifications are reflecting how the interference effects between the electron wavelengths and the chain length are destroyed. Our results have shown how the inelastic processes reduce the conductance and its oscillations as a function of the Fermi energy of the ideal chain. This is the expected result, since inelastic processes should eliminate the electron memory of its phase at a distance of the order of its inelastic mean free path.

We should comment that our analysis of the inelastic regime has been performed by including the electron–electron interaction explicity. Based on a self-energy local approximation we have shown that the inelastic processes can be described by means of an effective parameter, $\mathrm{Im}\langle\Sigma^{\mathrm{R}}\rangle$, that plays the role of an electron mean lifetime. Although the discussion has been concentrated on the electron–electron interaction case, as given by equation (3*a*), it should be commented on that similar arguments can be used to discuss the electron–phonon interaction case, equation (3*b*), and that one can obtain the same results as for the electron–electron interaction. The equations obtained for the inelastic regime can also be applied to the electron–phonon scattering case.

Although the inelastic analysis of section 3 has been presented for an inelastic mean free path, λ, much larger than the chain length, (this implies $n\,\mathrm{Im}\langle\Sigma^{\mathrm{R}}\rangle \ll t_0$), it is worth discussing the qualitative behaviour one expects for the conductance of a linear chain in the limit of shorter mean free paths. Let us mention here that the opposite limit, $\lambda \ll L$ (or equivalently $n\,\mathrm{Im}\langle\Sigma^{\mathrm{R}}\rangle \gg t_0$) can also be analysed using the Keldysh method and by considering the inelastic current, which turns out to be the only term contributing to the total current (the elastic current goes to zero in this limit, $\lambda \ll L$). Then one can show (details will be published elsewhere) that the

total current for $\lambda \ll L$ is given by the following equation:

$$G = I/(\mu_R - \mu_L) = (2e^2/h)(t_0 \sin\alpha/n\,\mathrm{Im}\langle\Sigma^R\rangle)\frac{4c\sin\alpha\sin\alpha'}{[1+c^2+2c\cos(\alpha-\alpha')]}. \quad (33)$$

This equation shows that for $\lambda \ll L$, the total conductance is inversely proportional to $n\,\mathrm{Im}\langle\Sigma^R\rangle$; this result yields Ohm's law for a one-dimensional system. The Ohm's law resistance is proportional to the inverse of the relaxation time $\mathrm{Im}\langle\Sigma^R\rangle$ owing to inelastic collisions, and to the inverse of the length of the linear chain.

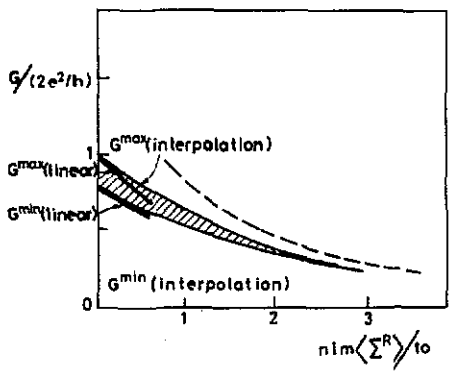

Figure 12. The qualitative behaviour of the linear-chain conductance, $G/(2e^2/h)$, as a function of $n\,\mathrm{Im}\langle\Sigma^R\rangle/t_0$. Equation (33) is shown by the broken curve.

A qualitative behaviour of the conductance of an ideal chain as a function of $n\,\mathrm{Im}\langle\Sigma^R\rangle/t_0$ is shown in figure 12, for the Fermi level located around the middle of the band width. The limit $n\,\mathrm{Im}\langle\Sigma^R\rangle/t_0 \ll 1$ corresponds to a very long mean free path; in figure 12 we represent the minimum and the maximum conductance, the shaded region corresponding to intermediate values depending on the exact position of the Fermi level. In the other limit, $n\,\mathrm{Im}\langle\Sigma^R\rangle \gg 1$, we recover Ohm's law. Although figure 12 shows a qualitative description of the ideal linear-chain conductance, notice that the long mean free path limit should disappear for $n\,\mathrm{Im}\langle\Sigma^R\rangle/t_0 \simeq 1$. Then we can expect that, for larger values of $n\,\mathrm{Im}\langle\Sigma^R\rangle/t_0$, the conductance oscillations and any other oscillatory properties such as the electrochemical potential variations discussed in this paper should disappear.

Acknowledgments

This work has been partially financed by the Spanish CICYT under contract MAT 89-165. This work was partially supported by the Universidade Federal Fluminense and the Brazilian CNP. We thank A Martin-Rodero for many interesting discussions and for his help in clarifying several results. We also thank F Sols for interesting discussions.

References

Altshuler B L, Aronov A G and Khmelnitsky D E 1982 *J. Phys. C: Solid State Phys.* **15** 7367
Anda E V and Flores F 1991 *J. Phys.: Condens Matter* **3** 9087

Binning G, Rohrer H, Gerber Ch and Weibel E 1982 *Phys. Rev. Lett.* **49** 57
Büttiker M 1985 *Phys. Rev.* B **32** 1846
—— 1988 *IBM J. Res. Dev.* **32** 317
—— 1989 *Phys. Rev.* B **40** 3409
Caroli C, Combescot R, Nozières P and Saint-Jones D 1971 *J. Phys. C: Solid State Phys.* **4** 916
D'Amato J L and Pastawsky H M 1990a *Phys. Rev.* B **41** 7411
—— 1990b *J. Phys.: Condens Matter* **2** 8023
Datta S 1990 *J. Phys.: Condens Matter* **2** 8023
Esaki L and Tsu R 1970 *IBM J. Rev. Dev.* **14** 61
Keldysh L V 1964 *Zh. Eksp.Teor. Fiz.* **47** 1515
Landauer R 1989 *J. Phys.: Condens Matter* **1** 8099
McLennan M J, Yong Lee and Datta S 1991 *Phys. Rev.* B **43** 13846
Pernas P L and Flores F 1991 *Physica* B **175** 221
Pernas P L, Martin-Rodero A and Flores F 1990 *Phys. Rev.* B **41** 8553
Rammer J and Smith H 1986 *Rev. Mod. Phys.* **58** 323
Sols F 1992 *Ann. Phys., NY* **214** 386
Stone D A and Szafer A 1988 *IBM J. Rev. Dev.* **32** 384